Egypt. J. Chem. **Vol. 67**, No. 1 pp. 37 - 55 (2024)

Egyptian Journal of Chemistry

http://ejchem.journals.ekb.eg/

Synthesis, characterization and anticancer potency of novel Mn(II), Co(II), and Cu(II) complexes based on N-[(1E)-1-(4-hydroxy-6-methyl-2-oxo-2H-pyran-3-yl)ethylidene]-2-(4-methylanilino)acetohydrazide

Fathy A. El-Saied [1], Tarek A. Salem [2], Alaa N. Metwaly [1], Bishoy El-Aarag [3,4,5,*]

[1] Chemistry Department, Faulty of Science, Menoufia University, Shebin El-Kom, Egyp, t[2] Molecular Biology Department, Genetic Engineering and Biotechnology Institute, University of Sadat City, Egypt, [3] Biochemistry Division, Chemistry Department, Faculty of Science, Menoufia University, Shebin El-Koom 32512, Egypt, [4] Division of Chemistry and Biotechnology, Graduate School of Natural Science and Technology, Okayama University, Okayama 7008530, Japan, [5] Center for Targeted Drug Delivery, Department of Biomedical and Pharmaceutical Sciences, Chapman University School of Pharmacy, Harry and Diane Rinker Health Science Campus, Irvine, CA 92618, USA

Abstract

Metal (II) complexes based on the ligand, N-[(1E)-1-(4-hydroy-6-methyl-2-oxo-2H-pyran-3-yl)ethylidene]-2-(4-methylanilino)acetohydrazide (HL) with Co (II), Mn (II), and Cu (II) were successfully synthesized and characterized by the use of analytical, spectral (IR, UV-vis, ^{1}H NMR), and thermal (TGA) measurements. Also, magnetic moment, molar conductance, and electron spin resonance (ESR) spectral assignments for Cu(II) complexes were measured. Moreover, the newly synthesized complexes were tested against Huh-7, HCT-116, A549 cancer cell lines using MTT assay. Their apoptotic activity was determined through flow cytometry using Annexin-V-FITC/PI. Moreover, their ability to arrest cell cycle was studied. Results revealed that the complex of Mn (II) is a high spin octahedral, cobalt (II) complexes are high spin tetrahedral, and copper (II) complexes are square planar. Also, Mn (II), Co (II), and Cu (II) complexes of the ligand showed cytotoxicity activity. The tested complexes showed cytotoxic activity towards three human cancer cell lines, particularly complexes 3 and 5. Complex 3 recorded IC_{50} values 10.51 µM and 24.96 µM, respectively against Huh-7 and A549 cells. Complex 5 showed IC_{50} values 28.86 µM and 7.2 µM, respectively against Huh-7 and A549 cells. Furthermore, results of the Annexin-V-FITC/PI apoptosis assay revealed that compounds could induce apoptosis in cancer cells by increasing the percentage of apoptosis. Complex 3 induces total apoptosis of 37.15% in Huh-7 cells while complex 5 gives 34.15% in A549 cells. Complex 3 gives a significant diminishing of cells in G0/G1 phase in HCT-116 cells, complex 5 caused less accumulation in G0/G1 phase in A549 cells. In conclusion, the new complexes exerted their anticancer activity through induction of apoptosis and cell cycle arrest of cancer cells.

Keywords: Dehydroacetic acid; hydrazone; metal (II) complexes; anticancer, apoptosis; cell cycle analysis

1. Introduction

Dehydroacetic acid (3-acetyl-4-hydroxy-6-methyl-2H-pyran-2-one) (DA) is an outstanding chelating agent. It has bactericidal, fungicidal, herbicidal, and insecticidal activities [1,2] in addition to its participation in the formation of extensive types of heterocyclic ring systems [3,4].

The interests for a long time in the synthesis and characterization of transition metals with ligands from the hydrazine family [5-14] and the Schiff base hydrazones formed usually by the action of hydrazine and ketones or aldehydes. They have been demonstrated to possess industrial, antifungal, antibacterial, antimicrobial [15], antitumor [16,17], herbicidal applications [18-20], antioxidant [21], anti-angiogenic [22], anti-convulsant [23], antitubercular [25], anti-inflammatory activities [26], and insecticidal activity that showed an effect on the percentage of larval mortality, pupation and adult emergence of the cotton leafworm Spodoptera littoral is treated as second larval instar by applying different concentration of the complexes [27–28] and the oral administration of vanadium complexes induced a significant hypoglycemic effect in

*Corresponding author e-mail: bishoy.yousef@gmail.com
Receive Date: 28 February 2023, Revise Date: 08 July 2023, Accept Date: 18 July 2023
DOI: 10.21608/EJCHEM.2023.196938.7652

diabetic rats [29]. Furthermore, some hydrazones have also been used as stabilizers and plasticizers for polymers [30,31] and hydrazones metal complexes have been used as catalysts [32–35]. So, some metal complexes of hydrazides have been synthesized and characterized [36–50].

Hydrazone derivatives are recognized for their wide range of biological activities [51,52]. A broad range of hydrazones have been applied as anticancer drugs including zorubicin and bisantrene. Sulfonyl hydrazone-substituted 8-ethoxy-3-nitro-2H-chromenes has been studied [53] which were active towards several cancer cell lines. Synthesized plumbagin hydrazone derivatives were active towards breast cancer [54,55]. Also, flurbiprofen hydrazide derivatives were active towards leukemia and ovarian cancer cell lines [56,57]. Also, definite compounds were synthesized and reported to possess antitumor activity towards MCF-7 cell lines [58, 59].

The antitumor activity of hydrazones-based compounds is induced through several manners, such as apoptosis, inhibition of angiogenesis and DNA intercalation. Several compounds also show their activity through cell cycle arrest. Stimulation of apoptosis is a good approach for the prevention of multiplication of cancer cells. Several hydrazones exhibited less toxic than hydrazides because of blockage of -NH_2 group. Consequently, hydrazones design with the aim to activate and promote apoptosis consider a crucial strategy in the development of potential anticancer agents such as (S)-2-(6-methoxynaphthalen-2-yl)-N'-{(E)-[2-(trifluoromethoxy)phenyl]methylidene}propanehydrazide which induce apoptosis and inhibit VEGFR-2 [60,61]. Furthermore, the tolmetinhydrazide-hydrazone with 2,6-dichlorophenyl moiety showed considerable cytotoxicity and apoptosis stimulation. Moreover, organotin (IV) complexes were reported with antibacterial activity [62–64]. In continuation to our interest [65,66] the current study aimed to prepare new metal (II) complexes derived from acetohydrazide ligand.

2. Materials and Methods

2.1. Instrumentation and measurements

Elemental Micro analyses [C, H, N] were evaluated in Micro Analytical Unit, Faculty of Science, Cairo University, Egypt. KBr discs on FT-IR Shimadzu spectrophotometer model spirit Fourier Transform Infrared spectrophotometer was used in the measuring the IR spectra. The ^{1}H NMR ligand spectrum has been recorded in DMSO-d6 on Varian Gemini 200 NMR spectrophotometer at 300 MHz. Mass spectrum ligand occurred on direct probe controller intel part to single quadropole mass analyzer in thermo scientific model (ISQLT) applying THERMO X-CALIBUR SOFTWARE. Electronic spectra in solid states in Nujol nulls and in N,N-dimethylformamide (DMF) solutions were recorded by the use of Schimadzu UV-Vis 1800 spectrophotometer. The molar conductance of (1 x10^{-3} M) solution of the complexes in N,N-dimethylformamide (DMF) had been estimated at 25 ºC by a Bibby conductometer type MCl. The resistance is measured in ohms and molar conductivities had been calculated by using this equation **{ Λ_M = VxKxg /Mw*Ω** } where: Λ_M = molar conductivity /$\Omega^{-1}cm^2mol^{-1}$, **V** = volume of the complex solution/ mL, **K** = cell constant (0.92/cm^{-1}), **Mw** = molecular weight of the complex, **g** = weight of the complex/g, **Ω** = resistance/**Ω**. The thermal analyses (TGA) were carried out under nitrogen applying Shimadzu DT-30 thermal analyser. Magnetic susceptibilities had been measured at 27 °C using the modified Gouy method with a Johnson Matthey balance. Magnetic moments were calculated using the following equation:

$$\{ \qquad \mu_{eff} = 2.84\sqrt{\chi_M^{corr}.T}$$

2.2. Preparation of ligand (HL)

Firstly, 4-methylaniline (1.07g, 10 mmol in 20 mL of ethanol) was added to a solution of ethylchloroacetate (1.22 g, 10 mmol in 40 mL of ethanol) to prepare ethyl(4-methylailino)acetate (m.p. = 43 °C). Secondly, to prepare 2-(4-methylanilino)acetohydrazide (m.p. = 162 °C), a solution of ethyl (4-methylanilino)acetate (1.79 g, 10 mmol) in 100 ml ethanol was added drop wise to a solution of hydrazine hydrate (2.5 g, 50 mmol). The mixture that obtained was refluxed by stirring for 3 h and left to cool at room temperature. The precipitate which formed was filtered off, washed with ethanol, and dried over anhydrous $CaCl_2$.

Finally, dehydroacetic acid (3-acetyl-4-hydroxy-6-methyl-2H-pyran-2-one (1.68 g, 10 mmol) in 30 mL ethanol was added drop wise to a solution of 2-(4-methylanilino)acetohydrazide (1.79 g, 10 mmol) in 100 mL ethanol. The formed mixture was refluxed with stirring for 3 h, then left to cool at room temperature. The obtained precipitate was filtered off, washed with ethanol, dried over anhydrous $CaCl_2$ as shown in Figure 1.

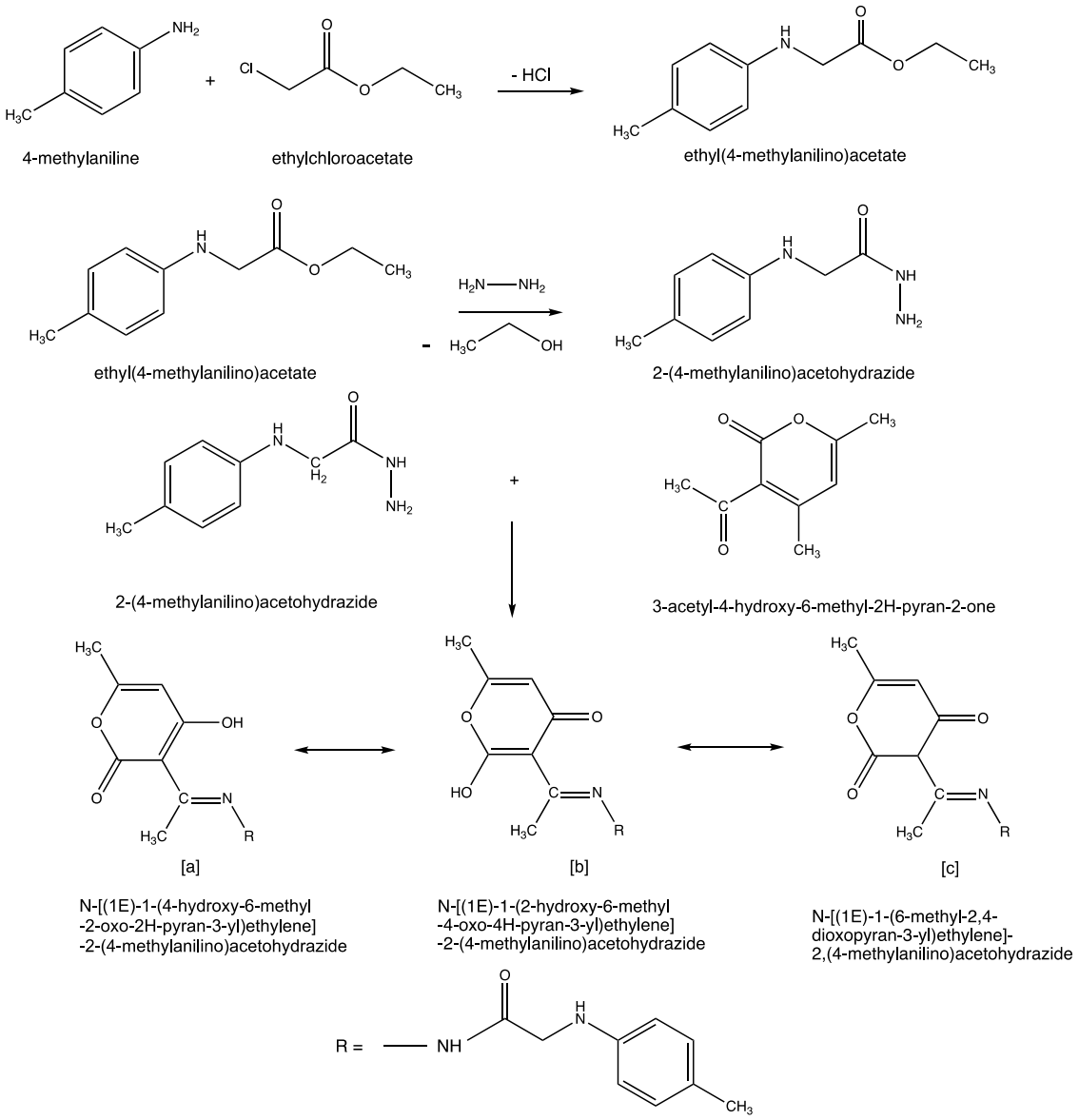

Figure 1: Preparation of ligand (HL) and the chemical formulations of its tautomeric forms [a], [b], and [c].

The ligand structure (Figure 1) has been elucidated according to the data of elemental analyses collected in Table 1, FT-IR spectral data listed in Table 2, ^{1}H NMR spectral data shown in Figure 2. The elemental analytical data agrees with the suggested formula. FT-IR spectral data of ligand displayed bands near 3354 (s), 3160 cm^{-1} and 3100 cm^{-1}, the first band is assigned to υ(4-C-O-H), the second two bands are assigned to imido -NH- groups [67]. The spectrum of the ligand also had shown bands in 1708, 1677 and 1612, assigned to υ(C=O) of lactone moiety (2-one carbonyl group) [67,68], υ(C=O) of hydrazine moiety, υ(C=N) of azomethine groups, respectively [69]. The presence of the band's characteristic to lactone (2-one) group and 4-C-OH and lack of bands characteristic to 4-one carbonyl group, have been taken as evidence

that the ligand exists mainly in the tautomeric form [a] shown in Figure 1.

As shown in Figure 2, ^{1}H NMR spectrum of ligand (HL) were recorded in DMSO-d6. The chemical shifts are given in ppm downfield from tetramethylsilane represented in Figure 2. Also, Figure 2 showed signals at 15.77 (1H, s, 4-C-OH), 11.11 ppm (1H, s, -CO-NH-), 6.42, 6.49 ppm (2H, d, CH) and 6.89, 6.91 ppm (2H, d, CH), these two doublet signals corresponding to the 4 aromatic protons of 1,4 disubstituted benzene [70]. The proton attached to the C5 carbon of dehydroacetic acid (DA) ring seemed like a sharp singlet at 5.87 ppm [71]. Methyl protons attached to C6 carbon seemed like a singlet at 2.15 ppm, whereas methyl protons attached to C4 of anilino moiety and azomethine carbon (C7) appeared at 2.45 and 2.11 ppm, consequently. Aliphatic protons (-CH_2) appeared at 3.93 ppm. A singlet signal characteristic to (1H, s, anilino-NH-) was observed at 3.3 ppm. The existence of the signal characteristic to (1H, s, 4-C-OH), and the appearance of band characteristic to the lactone carbonyl group in the infrared spectrum confirmed that the ligand exists mainly in tautomer [a] shown in Figure 1.

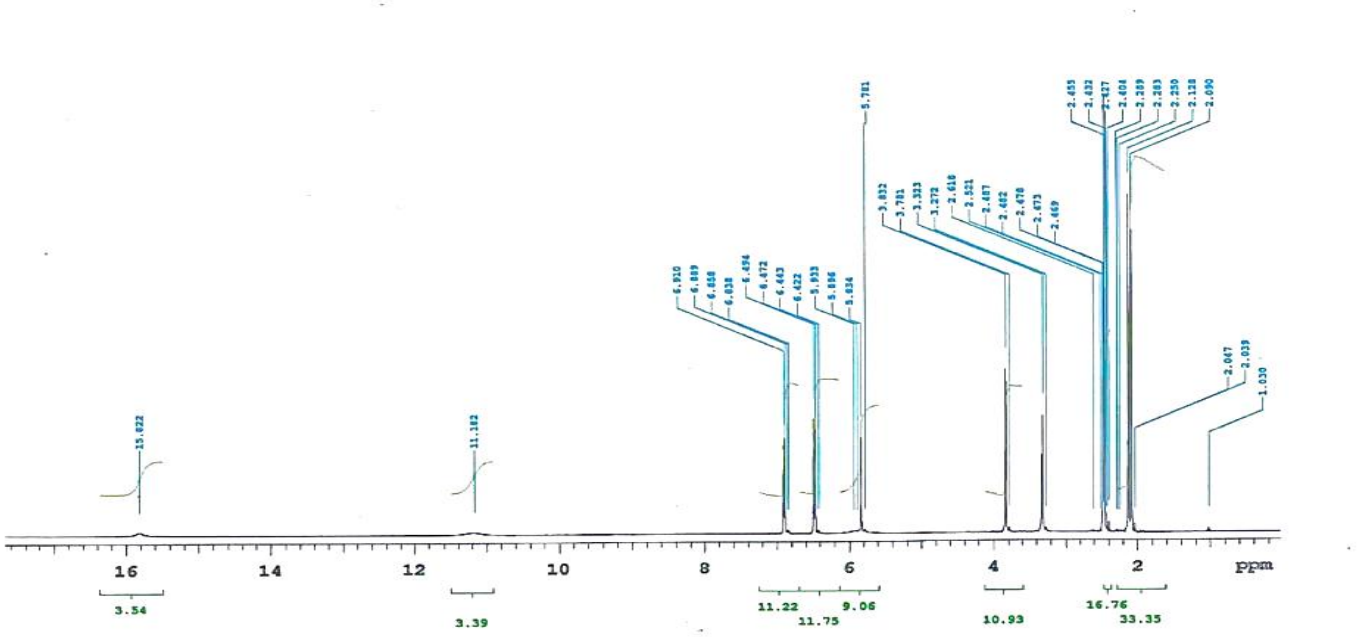

Figure 2: ^{1}H NMR spectrum of HL.

2.3. Preparation of metal (II) complexes (2-6)

Metal (II) complexes of ligand were prepared by mixing a hot ethanolic solution (30 cm^3) of metal salts: $Mn(OAc)_2$, $Co(OAc)_2.4H_2O$, $Co(NO_3)_2.H_2O$ $CuCl_2.2H_2O$ and $Cu(OAc)_2.H_2O$, with suitable amount of a hot ethanolic solution of ligand in 1:1, (ligand/metal) molar ratio. The reaction mixture was then refluxed for about 2 h. The formed precipitates had been filtered off, washed with ethanol, dried under vacuum over anhydrous $CaCl_2$. The chemical structures of complexes were shown in Figure 4.

2.4. Cell lines and cell cultures

Liver cancer Huh-7 cells, lung adenocarcinoma A549 cells, and colorectal carcinoma HCT-116 cells had been grown in Dulbecco's Modified Eagle's Medium (DMEM) with the supply of 10% fetal bovine serum (FBS) and 100 µg/mL kanamycin. The maintenance of cells was done at a 5% CO_2-humidified atmosphere at 37 °C and the replacing of the culture medium with new one was completed after couple of days. The cells were sub-cultured when the cell confluency reached about 80%.

Mass spectrum of ligand showed a peak at m/z 329 attributed to M^{+1} peak that corresponds to molecular weight of ligand 329 gram/mole as shown in Figure 3.

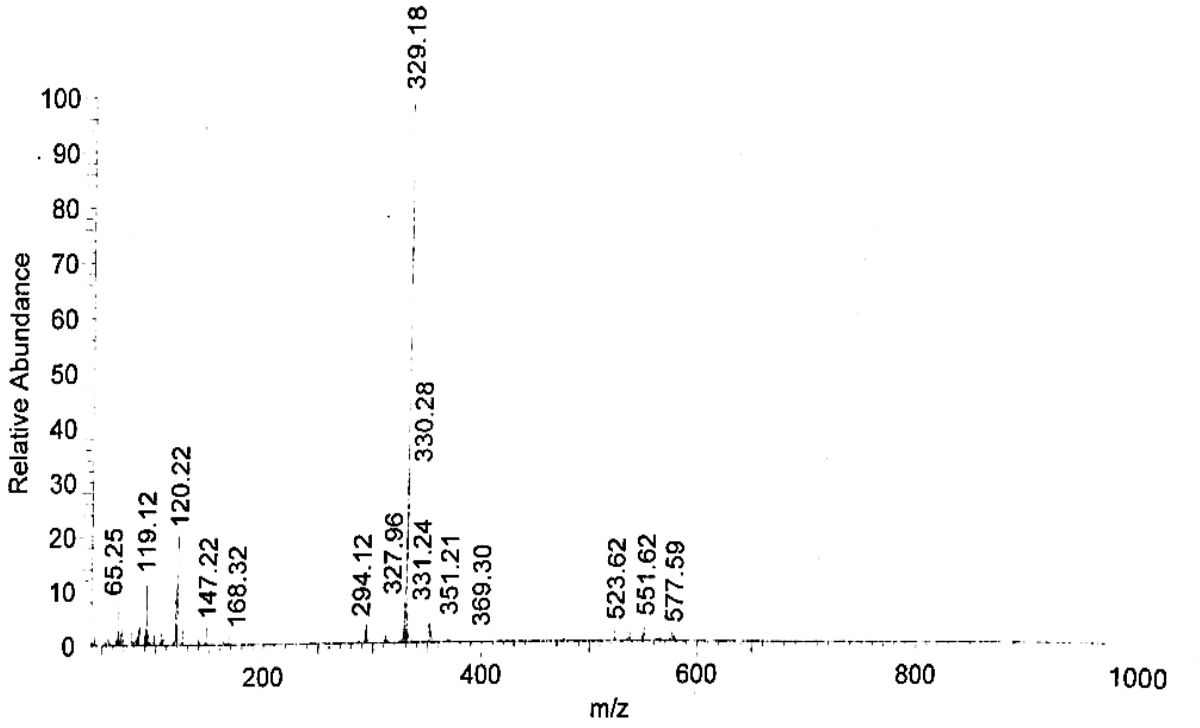

Figure 3: Mass spectrum of the ligand.

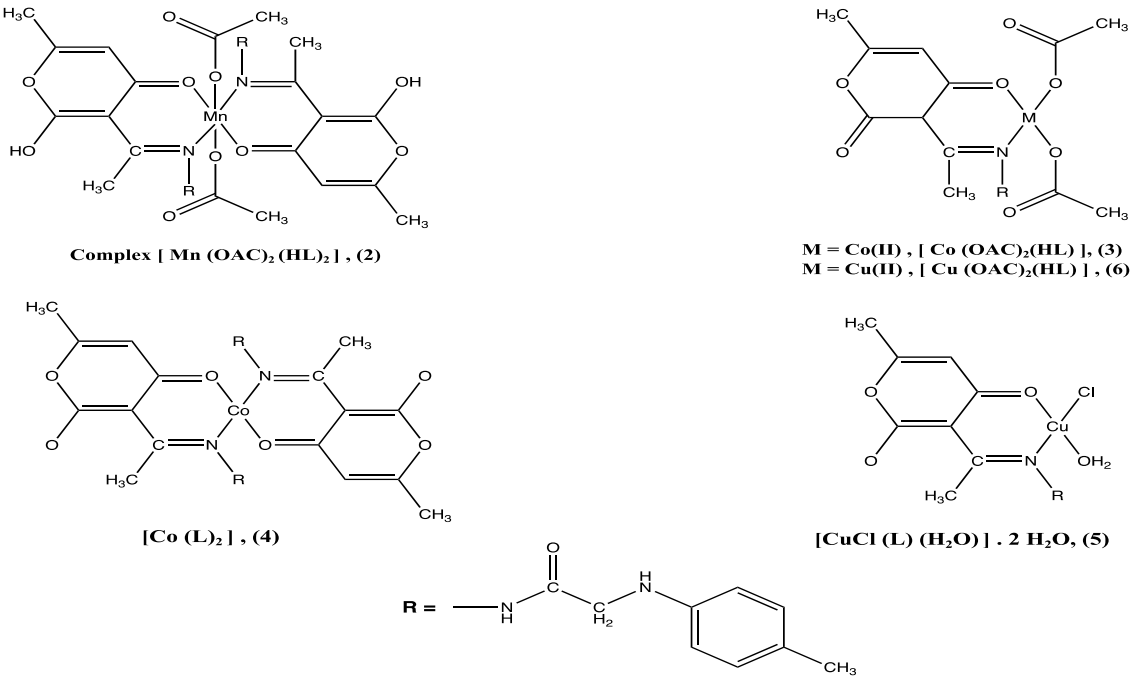

Figure 4: Chemical structures of metal (II) complexes (2–6)

2.5. Cell proliferation assay

The antiproliferative activity of acetyl hydrazone metal (II) complexes (6.25–100 µM) against Huh-7, A549 and HCT-116 cells had been evaluated through using 3-(4,5-dimethylthiazol-2-yl)-2, diphenyltetrazolium bromide (MTT) assay as described [72]. In brief, the cells at a density of 5 x103 cells/well in complete media had been seeded in 96-well plates. After 24 h of culture, complexes (6.25–100 mM) were individually added. Post 48 h, the cells had been subjected to MTT at a final concentration of 1 mg/mL for 4 h. A 10% SDS containing 0.02 N HCl had been used for dissolving the formed formazan crystals. A spectrophotometer at 570 nm was used to read the optical density.

2.6. Apoptosis assay

The apoptotic effect of acetyl hydrazone metal (II) derivatives (6.25–100 µM) against Huh-7, A549, and HCT-116 cells was determined [73] using Annexin V-FITC kit based on the manufacturer's instructions. In brief, cancer cells had been individually treated with complexes (IC_{50}) for 24 h. After twice washing of the cells with cold PBS, the cells were resuspended in 1 x binding buffer (1 $x10^6$ cells/ml). In the dark, 5 mL of Annexin V-FITC, 5 mL of PI had been added to cells and then samples had been vortexed, incubated at room temperature for 15 min. A binding buffer (1x, 400 mL) was added to tubes then samples were analyzed using flow cytometry.

2.7. Cell cycle analysis

The effect of acetyl hydrazone metal (II) complexes on Huh-7, A549 and HCT-116 cell cycle distribution was performed using Fluorescence Activated Cell Sorter (FACS). In brief, cells (2×10^5/well) had been seeded on 6-well plate and after 24h, the cells had been treated with ligand, complexes (IC_{50}) for 24 h. An ice-cold Ethanol: PBS (70:30, v/v) was used to fix the cells for 30 min at 4 °C. RNase, propidium iodide (PI) had been added to cells for 30 min with incubation at 37 °C. A FACSCalibur instrument equipped with FACS Calibur software was used to analyze the DNA content of 10,000 cells.

2.8. Statistical Analysis

The results of the assays were presented in the form of mean ± SD. One-way ANOVA, Tukey post hoc test had been used for analyzing statistical comparison among studied groups. A statistically significant had been considered at $p < 0.05$.

3. Results and Discussion

3.1. Characterization of metal complexes (2-6)

Ligand had been reacted with manganese (II), cobalt(II) and copper(II)) salts in 1;1 molar ratios , produced complexes listed in Table 1 and their chemical formulations were shown in Figure 4. Colors, elemental analyses, stoichiometry, molar conductivity of the prepared metal complexes were listed in Table 1. The obtained solid metal complexes are air stable and partially soluble in most organic solvents except N,N-dimethylformamide (DMF) and N,N-dimethylsulfoxide (DMSO) are completely soluble. The elemental analyses confirmed that the complexes (3, 5 and 6) include ligand and metal ions with molar ratios 1L:1M, whereas complexes 2 and 4 are formed in 2L:1M molar ratio. Analytical, physical, spectral data are suitable with suggested structures (Figure 2). Resulting complexes were characterized by different analytical, spectroscopic techniques such as ^{1}H NMR, FT-IR, UV-Vis spectra, magnetic moment, molar conductivity measurements in addition to elemental, TGA analyses.

3.2. The molar conductivity

The molar conductivities in DMF (10^{-3} M) at 25 °C of metal (II) complexes are listed in Table 1. Metal complexes 2–6 display molar conductivity values ranging from 11.95 to 19.24 $ohm^{-1}cm^2mol^{-1}$, indicating their non-electrolytic nature. This confirmed that anions in all these complexes are directly attached to metal ions [74–75].

3.3. Infrared spectra

IR spectra of complexes had been investigated, compared with that of the ligand for illustrating mechanism of bonding of ligand with several metal ions. The most diagnostic infrared spectral bands, their assignments were collected in Table (2). The band corresponding to υ(C=N) in spectra of all complexes shifts to lower wavenumber, showing that azomethine-nitrogen atom is existed in the coordination in all complexes [76-77].

Table (1): Yield, melting point, color, molar ratio, molecular weight, elemental analyses, and molar electrical conductivity of ligand and metal complexes.

NO	Compound	Yield %	M.P. °C	Molar ratio L:M	Color	Molecular weight g/mol	%C F (C)	%H F (C)	%N F (C)	Λ_M (a)
1	HL	--	210	–	pale yellow	329	61.54 (62.0)	6.11 (5.8)	13.00 (12.76)	--
2	$[Mn(OAc)_2(HL)_2]$	89	230	1:1	yellow	831.00	54.4 (54.87)	4.94 (5.29)	10.22 (10.10)	18.80
3	$[Co(OAc)_2(HL)]$	75	280	1:1	green	505.70	50.30 (49.83)	4.50 (4.90)	08.90 (8.30)	17.34
4	$[Co(L)_2]$	75	280	1:1	orange	714.90	56.80 (57.10)	5.07 (5.03)	11.74 (11.75)	11.95
5	$[CuCl(L)(H_2O)].H_2O$	80	220	1:1	brown	463	43.70 (44.06)	4.40 (4.75)	09.10 (9.07)	15.48
6	$[Cu(OAc)_2(HL]$	66	250	1:1	green	510.5	48.90 (49.36)	4.90 (4.89)	8.96 (8.23)	19.24

(a) = molar conductivity ($ohm^{-1}\ cm^2 mol^{-1}$); F: found (C) calculated.

The stretching vibration band of hydrazino-carbonyl group in the spectra of all metal complexes (2-6) observed at the same wavenumber or showed very slight shift in comparison with that of the free ligand, showing that hydrazino carbonyl group not participating in coordination to metal ion in all complexes. The infrared spectrum of the complex $[Mn(OAc)_2(Hl)_2]$ (2) showed that the band characteristic to υ(C=O) of lactone group disappeared, a strong band appeared at 3352 cm-1, assigned to υ(2-C-OH). Moreover, a band observed at 1615 cm^{-1}, was attributed to coordinated 4-one carbonyl group. These are evidence that the ligand bonded to the manganese(II) in the tautomer [b] shown in Figure 1. In this complex the ligand behaves like a neutral bidentate,
coordinated via the azomethine nitrogen atom and the 4-one carbonyl oxygen atom. The infrared spectra of complexes $[Co(OAc)_2(HL)]$ (3) and $[Cu(OAc)_2(HL)]$ (6) displayed the lactone band at 1705 and 1710 cm^{-1} respectively, at same position as that of the free ligand. Moreover, spectra of complexes 3 and 6 had shown bands at 1630 and 1625 cm^{-1}, respectively, referred to coordinated 4-one carbonyl group. The appearance of these two bands and lack of any bands corresponding to hydroxy group, have been taken as evidence that the ligand in these two complexes reacted to metal ion in the tautomer [c] (Figure 1) as a bidentate ligand coordinated via azomethine nitrogen atom and 4-one carbonyl (NO) mode. Infrared spectra of complexes $[Co(L)_2]$ (4) and $[CuCl(L)(H_2O)].H_2O$ (5) exhibited a band at 1614 cm^{-1}, assigned to coordinated υ(4-C=O). Infrared spectra of the two complexes did not show any bands characteristic to lactone carbonyl group (2-one), showing that the ligand in these two complexes reacted in tautomer [b] shown in Figure 1. The disappearance of the bands corresponding to υ(2-C-OH), indicating that the ligand deprotonated and reacted as a monobasic bidentate, coordinating through azomethine nitrogen atom and 4-CO (O4) oxygen atom, which is in agreement with our finding [66] for the complex of dehydroacetic acid N3-substituted 3-[Cu(DAhexim-H) Cl].MeCN, where DA is dehydroacetic acid and hexim is 3-hexamethyleneiminyl thiosemicarbazide), which studied by single crystal X-ray diffraction. The study showed loss of O2 proton, coordination has taken place via the O4, imine nitrogen and -S atom. The study showed also that the O4 has the shortest bond to copper (II) followed by imine-Cu and the S-Cu. distances are similar. Significant IR spectral surveys reported on metal acetate complexes [77], showed that acetate ligand coordinating to centre of the metal in a monodentate, bidentate or bridging manner. υa(-COO) and υs(-COO) of free acetate ions are at 1560, 1416 cm^{-1}, respectively. In monodentate υ(-C=O) is found at more high energy than υa(CO), υ(C-O) is lower than υs(-CO). Therefore, separation between two υ(C=O) bands is bigger in monodentate complexes than free ion. The reverse is noticed in bidentate acetate coordination. IR spectra of the acetato complexes 2, 3 and 6 showing two bands at (1595- 1579) and (1357-1352) cm^{-1}, assignable to υa (COO) and υs (COO), respectively. The variation between these two bands is about 243-227 cm^{-1}, the spectra exhibit a third band near 766 cm^{-1} assigned to δ(COO) shows that the acetate in these complexes can coordinate to the metal ion like a monodentate ligand [78]. The inclusion of one water molecule in the coordinated

sphere of metal complex 5 is dependent on the appeal of bands near 3380, 935 and 618 cm^{-1} due to υ(OH), ρrock(H_2O) , ρwagg(H_2O) respectively [79]. IR spectra of all metal complexes indicates two new bands at 618–583 and 551–531 cm^{-1}, assigned to υ(M-O) [80] and υ(M-N) [81], respectively.

Table (2): Infrared spectral bands, their assignments for ligand and Mn(II), Co(II), and Cu(II) complexes

No	Compound	υ(C-OH)	υ(N-H)	υ(C=O)[a]	υ(C=O)[b]	υ(C=O)[c]	υ(C=N)	υ(OAc)	υ(M-O)/ υ(M-N)
1	HL	3354 (s)	3160, 3100	1708	-	1677	1612	_	
2	$[Mn(OAc)_2(HL)_2]$	3352	3204(br)	-	1615	1666	1546	1995,1357	583/ 551
3	$[Co(OAc)_2(HL)]$	-	3244	1705	1630	1680	1544	1579, 1352	589/ 545
4	$[Co(L)_2]$	-	3207	-	1614	1666	1545	-	583/551
5	$[CuCl(L)(H_2O)].H_2O$	3380[d]	3200	-	1614	1665	1545	-	618/537
6	$[Cu(OAc)_2(HL]$	-	3243	1710	1625	1679	1543	1579,1352	585/ 534

[a]= lactone carbonyl group (2-one), [b]= 4- one carbonyl, [c]= hydrazone carbonyl group, [d]= υ(-OH) of water.

3.4. Electronic absorption spectra, magnetic moment of the ligand and metal complexes

The magnetic moment values per one metal atom (B.M) estimated at room temperature and electronic spectral data in solid and in DMF solutions were depicted in Table 3. The magnetic moment and electronic spectra go through light on the geometry of metal complexes. Data in Table 3 showed that electronic spectrum of ligand exhibited bands at 277, 315, 326, 355, and 370 nm. These bands are due to electronic transitions, π → π* of benzene rings, n → π* of the enolic functional group (C=C-OH), n → π* of the lactone carbonyl group of dehydraacetic acid, n→ π* of hydrazine carbonyl group and n → π* of the free azomethine group, respectively [82, 83]. Table 3 showed that the π→ π* does affect by complex formation, whereas the n→ π* showed shifts to lower or higher wavelength comparing with that of free ligand, due to participating of function groups in coordination. Electronic spectrum of Mn(II) complex in DMF solution showing two weak bands at 705 and 508 as well as a strong band at 410 nm, assignable to the transitions 6A1g →4T1g, 6A1g → 4T2g, charge transfer, respectively. The electronic transitions together with a magnetic moment value 5.95 B.M, which is close to the spin- only value (5.92 B.M) suggesting d5 high spin octahedral geometry for Mn(II) complex [84,85]. Cobalt(II) complexes (3,4) give a magnetic moment value 3.75, 3.71 B.M for metal ion respectively, that is agreement with higher spin tetrahedral cobalt(II) complexes [86]. The electronic spectrum for complex 3 shows a broad band with various features around 644 nm, assigned to 4A2→4T1(P) (v3) transition in a tetrahedral arrangement around Co(II) ion [86]. Spectrum showed two charges transfer bands at 400 and 415 nm. The spectrum of complex 4 exhibited the 4A2→4T1(P) (v3) band, as a high intensity multiple structured band (526, 516, 500 nm). The noticed splitting, higher intensity of this band confirms tetrahedral organizing around Co(II) ion [87]. Complex 4 showed two bands at 440 and 470 nm referred to charge transfer electronic transitions. Copper(II) complexes 5 and 6 display μeff values 1.81 and 1.85 B.M., respectively near to spin value 1.73 B.M. Complexes 5 and 6 show a broad band at 650, 630 nm respectively which is assignable to the transition 2B1g → 2Eg, confirming a square planar geometry [88, 89] around copper(II) ion. Complex 5 showed two strong bands at 440, 460 nm, whereas complex 6 showed one strong band at 466 nm. These bands are assigned to charge transfer electronic transitions.

Table (3): Magnetic moment values, electronic spectral bands, and their assignments for ligand and metal (II) complexes.

No	Compound	υ(π→π*)	υ(n→π*)	Charge transfers electronic transitions	d→d electronic transitions	$\mu_{eff.\ (B.M.)}$ per one metal ion
1	HL	277	315, 326, 355, 370	-	-	-
2	$[Mn(OAc)_2(HL)_2]$	274	286, 324, 389,	410	580(w), 708(w)	5.95
3	$[Co(OAc)_2(HL)]$	274	292, 310, 324, 330	400 ,415	644 (br)	3.75
4	$[Co(L)_2]$	272	295, 328, 354, 377	440, 470	500, 516, 526	3.71
5	$[CuCl(L)(H_2O)].H_2O$	270	295,318 ,343, 390	440(br), 460(sh)	650(br)	1.81
6	$[Cu(OAc)_2(HL]$		303, 320 332,396	466(br)	630 (br)	1.85

3.5. Thermal analysis of metal (II) complexes

The TGA results for the solid ligand and its complexes (2–6) had been listed in Table 4. Results indicate a perfect harmony with formulae suggested from analytical, spectral, and magnetic data (Figure 4). Generally, the ligand and complexes 2,3,4, and 6 show thermal stability up to 220 ˚C, 215 ˚C, 250 ˚C, 260 ˚C, and 230 ˚C, respectively. The TAG thermograms of complexes 2, 3 and 6 displayed loss weight ranging from 215–290 ˚C, 250–345 ˚C, and 300–332 ˚C, corresponding to loss of two acetate groups.

Complex 5 displayed a weight loss from 44.37–150 ˚C and 151–327 ˚C, the first loss attributed to loss of one mole hydrated water and the second loss because of loss of one mole coordinated water and one chloride. The TGA thermograms of compounds (1-6) showed thermal decomposition to the corresponding metal oxide and carbon residue within the temperature ranges 220–600 ˚C, 290–430 ˚C, 345–460 ˚C, 260-500 ˚C, 322–600 ˚C, and 333–475 ˚C, consequently. TGA thermograms for metal (II) complexes 3 and 5 were proved in Figures 5 and 6 while the rest of the TGA thermograms were presented in the supplementary file in Figures S1–S4.

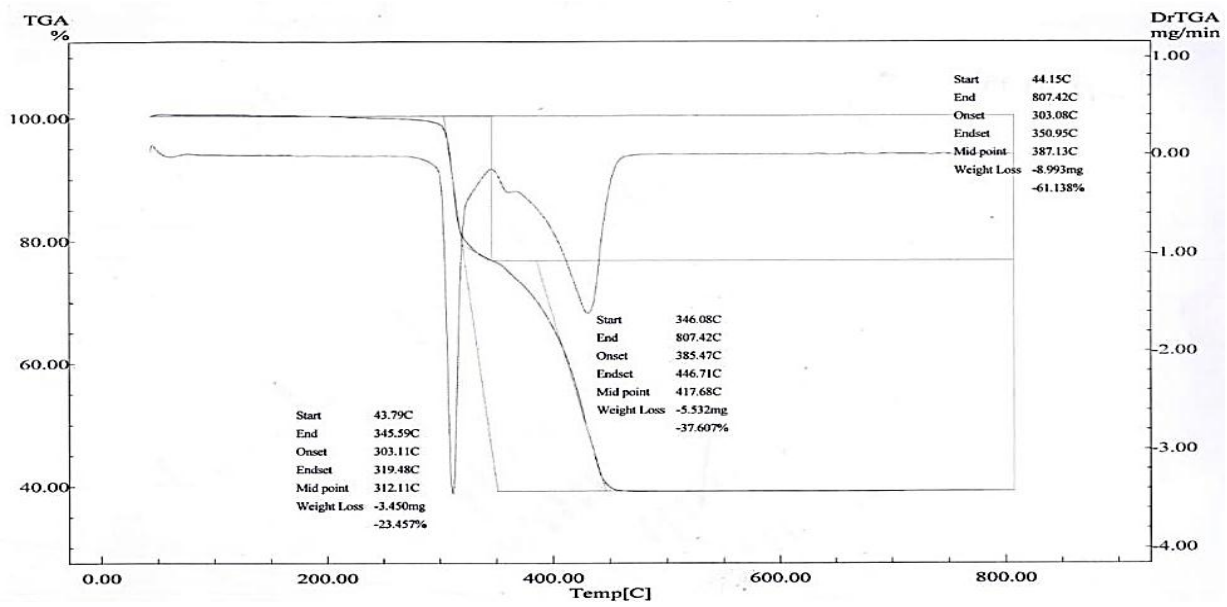

Figure 5: TGA for $[Co(OAC)_2\ (HL)]$ (3)

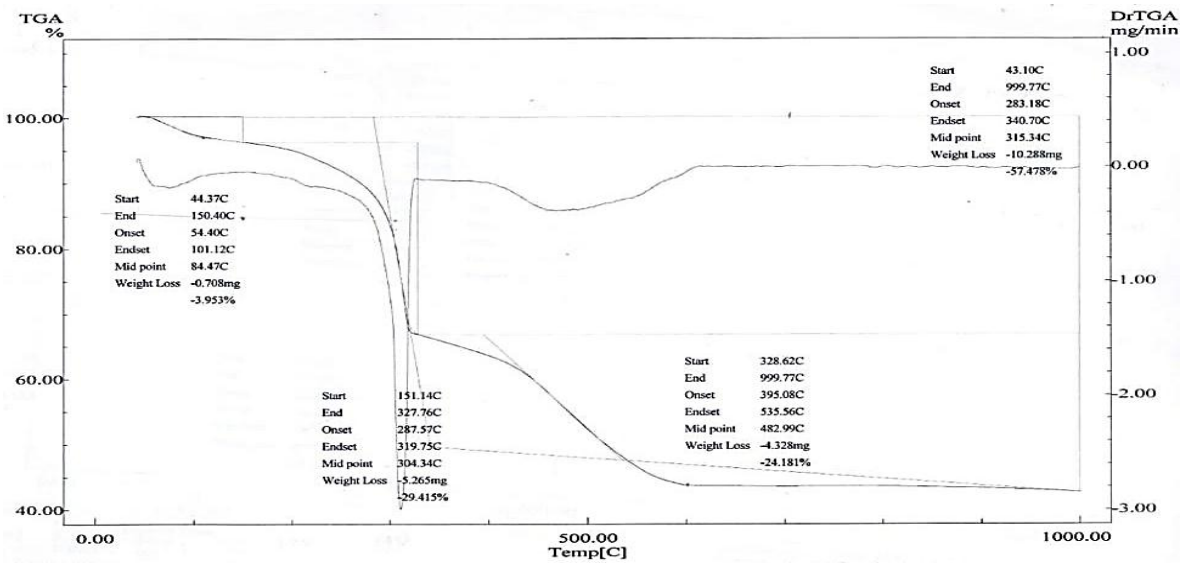

Figure 6: TGA for $[CuCl(L)(H_2O)].H_2O$ (5)

Table (4): TGA data for ligand, complexes, and their assignments.

No.	Compound	Temp. range (˚C)	Weight loss Found (calc)%	Assignment	Residual's formula
1	HL	220 220–600	zero 82.4(82.0)	thermal stability up to 220˚C complete decomposition of ligand to C	HL 5C
2	$[Mn(OAc)_2(HL)_2]$	0–215 215–290 290–430	zero 14.66(14.0) 55.20(55.0)	Thermal stability up to 215 ˚C Loss of 2OAc group decomposition of complex to Mn_2O_3 and C	$[Mn(OAc)_2(HL)_2]$ $[Mn(HL)_2]^{2+}$ Mn_2O_3 +8C
3	$[Co(OAc)_2(HL)]$	0–250 250–345 345–460	zero 23.45(23.1) 37..67(38.5)	Thermal stability up to 250 ˚C Loss of (2OAc) decomposition of complex to CoO and C	$[Co(OAc)_2(HL)]$ $[Co (HL)]^{2+}$ CoO +10 C
4	$[Co(L)_2]$	0–260 260–500	zero 58.9 (58.0)	Thermal stability up to 260 ˚C decomposition of complex	$[Co(L)_2]$ CoO +19 C
5	$[CuCl(L)(H_2O)].H_2O$	44.37–150 151–327 322–600	3.95(4.00) 12.63(12.00) 42.50(43.00)	Loss of hydrated water (H_2O) Lossing of coordinating water + Cl decomposition of complex forming metal oxide, carbon	$[CuCl(L)(H_2O)].$ $[Cu(L)]^+$ CuO +10C
6	$[Cu(OAc)_2(HL]$	0–230 300–332 333–475	zero 25.73(25.00) 41.00(41.00)	Thermally sable up to 230 ˚C loss of 2 OAc decomposition of complex formation to copper oxide and carbon	$[Cu(OAc)_2(HL]$ $[Cu(HL)]^{2+}$ CuO + 8C

3.6. Electron spin resonance (ESR) spectra of copper(II) complexes

The ESR spectra of the copper(II) complexes were recorded with X-band EMX spectrometer (Bruker, Berlin, Germany) using a standard rectangular cavity of ER 4102 operating at 9.5 GHz with 100 kHz modulation at 298 °K. Ag-marker for the calibration of the spectra was diphenylpicrylhydrazide (DPPH). The ESR spectra for Cu(II) complexes provides more information about their geometry. The ESR data of Cu(II) complexes 5 and 6 in the polycrystalline state at 298 K are listed in Table 5. The ESR spectrum of complex 5 (Figure 7), shows rhombic type distortion with three g-values g3(g‖) = 2.7149, g2= 2.2101, and g1 = 1.79. g⊥= (g1 +g2)/2 = (2.2101+1.79)/2 = 2.00002. The rhombic symmetry for this complex is attributable to the bulkiness of the ligand and to the unequal bond lengths of the four Cu-O, Cu-N, Cu-OH_2, and Cu-Cl [90]. The g tensors g3>g2>g1, indicative of complexes with d(x2−y2) ground state. This is also supported by the value of R factor R=(g2-g1/(g3-g2) < 1 (= 0.8322), confirming a d(x2–y2) ground state [91,92].

The ESR spectrum for complex 6 (Figure 8) demonstrates anisotropic signals with g‖>g⊥>2.0023 which are distinctive of an axial symmetry type of a d(x2-y2) ground state, resulting in a 2B1g ground state that is known for Cu^{2+} complexes [93,94]. These g-values support that the Cu^{2+} complex 6 has a square-planar geometry [95,96] The geometric parameter G, which is a measure of the exchange interaction between the copper centers in the solid state, is calculated using the equation G=(g‖-2.0023)/(g⊥-2.0023)=(2.7150-2.0023)/(2.006-20023)=57.5 for axial spectra. If G>4, exchange interaction is negligible and if it is less than 4, considerable exchange interactions exist [93,97]. The value of G>4, indicating that exchange interaction is negligible. Kivelson and Neiman have reported that the g‖-values for Cu^{2+}-complexes can be used to identify the nature of copper-ligand bonding. If the g‖-value is smaller than 2.3 an environment is essentially covalent, while if the value is larger than 2.3 the environment is essentially ionic [98]. For complexes 5 and 6, the g‖>2.3 denoting that there a considerable ionic character for copper-ligand bonding.

Table (5): ESR spectral assignments and bonding parameters for Cu(II) complexes in polycrystalline state at 298K.

Complex no.	$g_{\|}$ or g_3	$g_{\perp}$ or g_2 , g_1	$g_{\perp}$	g_{av}	G	R
[CuCl(L)(H_2O)].(H_2O) (5)	2.7149	2.2101, 1.79	2.00002	2.2383	-	0.8322
[$Cu(OAC)_2$(HL)] (6)	2.7150	-	2.006	2.2389	57.5	-

(-): no value available

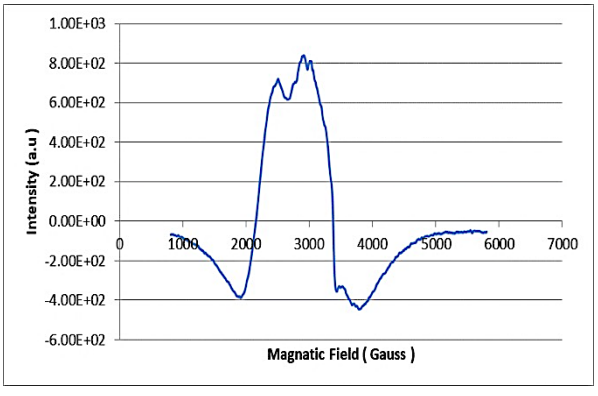

Figure 7: ESR for [CuCl(L)(H_2O).(H_2O)] (5)

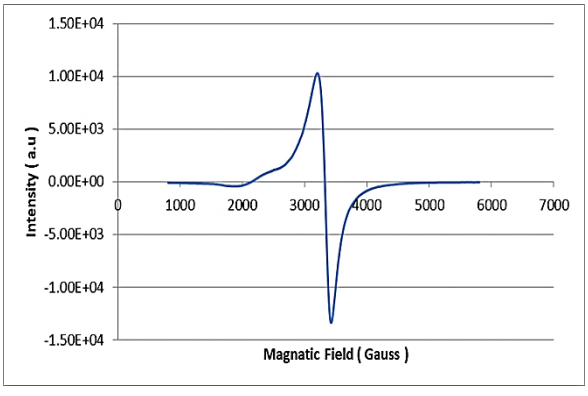

Figure 8: ESR for [$Cu(OAC)_2$(HL)] (6)

3.6. Biological activity

3.6.1. Cytotoxicity of the ligand and metal complexes against cancer cell lines

Ligand and metal complexes had been investigated against Huh-7, A549, HCT-116 cell lines through MTT assay. The IC_{50} values are reported in Table (6).

3.6.1.1. Cytotoxicity of ligand and metal complexes against Huh-7 cells

The most cytotoxic complex was complex 3 with recorded IC_{50} value 10.51 µM. The IC_{50} values for Complexes 5 and 6 were (28.86 µM), (13.32 µM), respectively. Complex 4 didn't show cytotoxic effect and its IC_{50} value was 1726 µM compared to ligand (1074 µM), and doxorubicin (55.94 µM) as shown in Table (6).

3.3.1.2. Cytotoxicity of ligand and metal complexes against A549 cells

As illustrated in Table (6) and concerning A549 cells, the IC_{50} results showed that the most cytotoxic complex was complex 5. It gave IC_{50} value (7.204 µM). The IC_{50} valued for complex 3 and 6 were (24.96 µM) and (46.11 µM), respectively compared to ligand (75.05 µM), and doxorubicin (10.1 µM).

3.6.1.3. Cytotoxicity of the ligand and metal complexes against HCT-116 cells

Relate to HCT-116 cells, the IC_{50} values showed that the most cytotoxic complex was complex 3 with IC_{50} value (30.49 µM). The IC_{50} for complexes 5 and 6 were (45.74 µM), and (34.91 µM), respectively while complex 2 showed the least cytotoxic activity (142 µM), compared to ligand (105 µM) and doxorubicin (27.7 µM) as shown in Table (6).

Table (6): IC_{50} values (µM) for ligand and complexes against Huh-7, A549, and HCT-116 cancer cell lines.

No.	Compound	IC50 (µM)		
		Huh-7	A549	HCT-116
1	Ligand (HL)	1074 ± 1.52	75.05 ± 2.02	105 ± 2.18
2	$[Mn(OAc)_2(HL)_2]$	77.18 ± 1.38	33.63 ± 1.09	142 ± 2.72
3	$[Co(OAc)_2(HL)]$	10.51 ± 1.88	24.96 ±2.08	30.49 ± 1.08
4	$[Co(L)_2]$	1726 ± 2.51	26.89 ±1.03	65.15 ± 2.13
5	$[CuCl(L)(H_2O)].H_2O$	28.86 ± 1.54	7.20 ±1.08	45.74 ± 1.59
6	$[Cu(OAc)_2(HL]$	13.32 ± 1.94	46.11 ± 2.08	34.91 ± 1.40
Reference drug	Doxorubicin	55.94 ± 2.01	10.10 ± 1.09	27.70 ± 1.63

3.7. Apoptotic activity of metal complexes

The ability of ligand and metal (II) complexes to induce apoptosis in Huh-7, A549, and HCT-116 cells had been determined by flow cytometry using Annexin V, propidium iodide (PI) dual staining. Cancer cells had been treated with ligand and its metal complexes at IC_{50} values for 24 h.

3.7.1. Apoptotic activity of ligand and complexes against HCT-116 cells

In HCT-116 cell, all the synthesized metal (II) complexes showed apoptotic activity more than that found in ligand (6.85%). Complex 3 increased apoptosis two-fold (19.03%) compared to ligand. The recorded apoptotic effect for complexes 5 and 6 was 13.61% and 9.77%, respectively as shown in Table (7).

Table (7): Apoptotic activity of ligand and complexes against HCT-116 cells

Compound	HCT-116 cell apoptosis			Necrosis
	Total	Early	Late	
Ligand (1)	6.85 ± 0.46	0.73 ± 0.03	4.05 ± 0.46	2.07 ± 0.46
Complex (3)	19.03 ± 0.32	1.79 ± 0.18	14.16 ± 0.43	3.08 ± 0.44
Complex (5)	13.61 ± 0.29	1.19 ± 0.15	8.50 ± 0.35	3.92 ± 0.36
Complex (6)	9.77 ± 0.36	2.15 ± 0.13	4.99 ± 0.33	2.63 ± 0.32
Doxorubicin	35.94 ± 0.19	1.64 ± 0.15	23.11 ± 0.31	11.19 ± 0.41
Control cells	2.47 ± 0.09	0.48 ± 0.04	0.13 ± 0.05	1.86 ± 0.07

3.7.2. Apoptotic activity of ligand and complexes against Huh-7 cells

Results in Table (8) illustrated that the complexes 3, 5, and 6 possessed an apoptotic ability to induce apoptosis in Huh-7 cells more than that found in ligand (5.42%). Complex 3 is the most effective complex to induce apoptosis (37.15%) compared to the reference drug (doxorubicin) followed by complex 6 (31.03). Complex 5 induces apoptosis by almost three-fold (16.47%) compared to ligand.

Table (8): Apoptotic activity of ligand and complexes against Huh-7 cells.

Compound	Huh-7 cell apoptosis			Necrosis
	Total	Early	Late	
Ligand (1)	5.42 ±0.24	0.92 ± 0.03	3.19 ± 0.78	1.31 ± 0.23
Complex (3)	37.15 ± 0.23	2.91 ± 0.11	26.88 ± 0.65	7.36 ± 0.19
Complex (5)	16.47 ± 0.13	3.41 ± 0.08	6.84 ± 0.55	6.22 ± 0.18
Complex (6)	31.03 ± 0.12	2.76± 0.07	12.96 ± 0.47	15.31 ± 0.10
Doxorubicin	38.11 ± 0.11	2.52 ± 0.06	22.64 ± 0.36	12.95 ± 0.05
Control cells	2.09 ± 0.08	0.63 ± 0.06	0.28 ± 0.13	1.18 ± 0.05

3.7.3. Apoptotic activity of ligand and complexes against A549 cells

Compared with the apoptotic activity of doxorubicin (39.21%), complex 5 had the most potent apoptotic ability towards A549 cells (34.15%) among the synthesized complexes. The apoptotic activity of ligand was 9.31%, while complex 3 and 6 induce apoptosis by 11.82% and 6.01%, respectively as demonstrated in Table (9). Our results are compatible with that previously reported which indicated the antiproliferative activity and apoptosis mechanism of new arene Ru(ii) carbazole-based hydrazone complexes [99].

Table (9): Apoptotic activity of ligand and complexes against A549 cells.

Compound	A549 cell apoptosis			Necrosis
	Total	Early	Late	
Ligand (1)	9.31 ± 0.29	1.41 ± 0.27	3.72 ± 0.18	4.18 ± 0.78
Complex (3)	11.82 ± 0.17	1.08 ± 0.24	7.59 ± 0.45	3.15 ± 0.65
Complex (5)	34.15 ± 0.11	5.03 ± 0.21	20.71 ± 0.36	8.41 ± 0.55
Complex (6)	6.01 ± 0.085	0.77 ± 0.19	3.28 ± 0.26	1.96 ± 0.47
Doxorubicin	39.21 ± 0.072	3.49 ± 0.14	16.65 ± 0.12	19.07 ± 0.36
Control cells	1.95 ± 0.061	0.61 ± 0.06	0.22 ± 0.07	1.12 ± 0.13

3.8. Cell Cycle Distribution Analysis

For determining the effect of ligand and complexes on cell cycle, three human cancer cell lines (HCT -116, Huh-7 and A549) were stained with PI, the cell cycle analyzed using flow cytometry.

3.8.1. Cell cycle distribution analysis of HCT-116 cells treated with ligand and complexes

The impact of metal complexes on cell cycle distribution had been investigated in HCT-116. Control cells had been found in G0/G1 phase (43.85%), S phase (42.41%), and G2/M phase (13.74%). Pre-G0/G1 population percentage shows apoptosis rate of cells that were found in accordance with the flow cytometry analysis results of apoptosis assay. Cells treated with ligand and complex 3 showed various patterns than control cells for G0/G1 phase (44.14% and 35.94%), S phase (43.61% and 54.15%), and G2/M phase (12.26% and 9.91%), respectively (Table 10). The data showed that, in cells treated with complex 3, the percentage of cells in G0/G1 phase declined almost 8% related to the values for ligand. Conversely, complex 5 enhanced the percentage of cells in G2/M phase approximately 8% compared to the values for ligand. Therefore, complex 3 directed a marked lessening of cells in G0/G1 phase, and complex 5 produced much growth in G2/M phase in HCT-116 cells.

3.8.2. Cell cycle distribution analysis of Huh -7 cells treated with metal (II) complexes

In Huh-7 cells, metal complexes showed an effect on cell cycle distribution where control Huh-7 cells showed percentages of G0/G1, S, and G2/M phases were 39.81%, 49.26%, and 10.93%, respectively compared to that found in ligand 43.61%, 47.36%, and 9.03%.

Table (10): Cell cycle distribution of HCT-116 cells treated with ligand and complexes.

Compound	Cell cycle phases (HCT- 116 Cells)			
	%G0-G1	%S	%G2/M	%Pre-G1
Ligand (1)	44.13 ± 0.59	43.61 ±1.32	12.26 ± 2.29	6.85 ± 1.30
Complex (3)	35.94 ± 1.23	54.15 ± 0.74	9.91 ± 2.32	19.03 ± 1.44
Complex (5)	41.36 ± 0.89	38.07 ±1.32	20.57 ± 1.32	13.61 ± 0.36
Complex (6)	42.54 ± 1.36	41.32 ± 0.37	16.14 ± 0.88	9.77 ± 0.79
Doxorubicin	29.86 ± 0.89	24.25 ± 0.99	45.89 ± 1.16	35.94 ± 1.45
Control cells	43.85 ± 0.68	42.41± 0.74	13.74 ± 0.19	2.47 ±1.32

On the other hand, cells treated with complexes 3 and 5 exhibited unique distribution than control cells for G0/G1 phase (41.52% and 31.88%), S phase (56.29% and 44.26%), and G2/M phase (2.19% and 23.86%), respectively. This data suggests that complex 3 leading to elevation of cells in G0/G1 phase and triggered a reduced amount of G2/M phase in Huh-7 cells as shown in Table (11).

Table (11): Cell cycle distribution of Huh-7 cells treated with ligand and complexes.

Compound	Cell cycle phases (Huh -7 cells)			
	%G0-G1	%S	%G2/M	%Pre-G1
Ligand (1)	43.61 ± 0.72	47.36 ± 0.69	9.03 ± 0.72	5.42 ± 0.58
Complex (3)	41.52 ± 0.44	56.29 ± 1.83	2.19 ± 1.68	37.15 ± 1.00
Complex (5)	31.88 ± 0.58	44.26 ± 1.69	23.86 ± 1.01	16.47 ± 0.89
Complex (6)	36.23 ± 1.01	42.51 ± 1.92	21.26 ± 1.48	31.03 ± 1.00
Doxorubicin	44.59 ± 0.76	51.26 ± 1.26	4.15 ± 1.01	38.11 ± 0.44
Control cells	39.81 ± 0.58	49.26 ± 1.51	10.93 ± 1.01	2.09 ± 0.96

3.8.3. Cell cycle distribution analysis of A549 cells treated with ligand and complexes

As shown in Table (12), metal (II) complexes exerted an effect on A549 cell cycle distribution. The results revealed that in control cells, the percentages were 54.72%, 39.25, and 6.03% for G0/G1, S, and G2/M phases, respectively comparing with that found for ligand 55.21%, 41.12%, and 3.67%. Cells treated with complex 3 showed a distribution pattern for G0/G1 phase (46.31%), S phase (38.56%), and G2/M phase (15.13%). In cells treated with complex 5, the cells proportion in G0/G1 phase was 42.62% and reduced nearly 12% compared with values for ligand (55.21%). Also, complex 5 conducted a significant decline of cells in G0/G1 phase (2.12%) compared to 5.01% in doxorubicin. These findings are compatible with complexes derived from hydrazone that exhibited an in vitro anticancer activity mediated by cell cycle arrest at the G2/M phase [100].

Table (12): Cell cycle distribution of A549 cells treated with ligand and complexes.

Compound	Cell cycle phases (A549 cells)			
	%G0-G1	%S	%G2/M	%Pre-G1
Ligand (1)	55.21 ± 0.93	41.12 ± 0.66	3.67 ± 0.69	9.31 ± 0.75
Complex (3)	46.31 ± 1.25	38.56 ± 0.76	15.13 ± 0.83	11.82 ± 0.48
Complex (5)	42.62 ± 0.93	55.26 ± 1.00	2.12 ± 0.69	34.15 ± 0.78
Complex (6)	52.13 ± 0.8	42.39 ± 0.66	5.48 ± 0.92	6.01 ± 1.01
Doxorubicin	36.85 ± 0.95	58.14 ± 0.58	5.01 ± 1.26	39.21 ± 0.76
Control cells	54.72 ± 0.71	39.25 ± 0.74	6.03 ± 0.51	1.95 ± 0.58

4. Conclusion

Mn(II), Co(II), and Cu(II) complexes of ligand were prepared and characterized. The results of analytical, magnetic susceptibility and electronic measurements reveal that the Mn(II) display octahedral geometry. The cobalt(II) complexes exhibit tetrahedral geometry. Copper(II) complexes are square planar. TGA of ligand and metal complexes agreed with the suggested structures for complexes. The tested complexes showed cytotoxic

activity towards three human cancer cell lines, particularly complexes 3 and 5. Furthermore, compounds could induce apoptosis in cancer cells by increasing the percentage of apoptosis. Complex 3 induces total apoptotic % of 37.15% in Huh-7 cells while complex 5 gave 34.15% in A549 cells. Complex 3 provides a significant reduction of HCT-116 cells in G0/G1 phase, complex 5 causing less accumulation in G0/G1 phase in A549 cells. The novel complexes exerted their anticancer activity through apoptosis induction and cell cycle arrest of cancer cells.

5. Conflict of Interest

The authors declare no conflict of interest.

6. Source of Funding

This research did not receive any specific grant from funding agencies in the public, commercial, or not-for-profit sectors

7. References

[1] Schleiffenbaum B., Spertini O., Tedder Thomas F., Soluble L-selectin Is Present in Human Plasma at High Levels and Retains Functional Activity, *J. Cell. Biol*., **119** (1), 229-234 (1992).

[2] Stanley G., Woldesenbet S., Cassandra G., Synthesis, characterization, thermal and 3D molecular modeling studies of transition metal complexes supported by ONN / ONO tridentate Schiff base hydrazone, *Poultry Sci*., **75** (1), 42-55 (1996).

[3] Munde A.S., Jagdale A.N., Jadhav S.M., Chondhekar T.K., Synthesis, characterization and thermal study of some transition metal complexes of an asymmetrical tetradentate Schiff base ligand. *J. Serb. Chem. Soc*., **75** (3), 349- 356 (2010).

[4] Levai A., Jeko J., Synthesis of 1,5-Disubstituted 3-(4-Hydroxy-6-methyl-2-oxo-2Hpyran-3-yl)-2-pyrazolines *Monatshefte für Chemie*., **137** , 339-345 (2006).

[5] Savanini L., Chiasserini L., Gaeta A., Pellerano C., Synthesis and anti-tubercular evaluation of 4-quinolylhydrazones, *Med. Chem*., **10**, 2193 (2002).

[6] Anten J.A., Nicholis D., Markopoulos J.M. Markopoulou O., Transition-metal complexes of hydrazones derived from 1,4-diformyl- and 1,4-diacetylbenzenes, *Polyhedron*, **6**(5),1075-1080 (1987).

[7] Singh M., Aggarwal V., Singh U.P., Singh N.K., Synthesis, spectroscopic and crystal structure investigation of [Cu(bzsmp)2Cl2] ; {bzsmp = 2-benzylsulfanyl-5-(2-methoxyphenyl)-1,3,4-oxadiazole}:cyclization of N 2-[bis(benzyl-sulfanyl)methylene]-2-methoxybenzohydra-zide to 2-benzylsulfanyl-5-(2-methoxyphenyl)-1,3,4-oxadiazole during complexation, *Polyhedron*, **28**, 195-199 (2009).

[8] Tossidis I.A., Bolos C.A., Aslanidis P.N., Katsoulos G.A., Monohalogenobenzoyl-hydrazones Synthesis and Structural Studies of Pt(II), Pd(II) and Rh(III) complexes of Di-(2-pyridyl) ketonechlorobenzoyl hydrazones, *Inorganica Chimica Acta*, **133**(2), 275-280 (1987).

[9] Sahebalzamani H., Ghammamy S., Mehrani K., Salimi F., Synthesis, characterization and thermal analysis of Hg(II) complexes with hydrazide ligands, *Der Chemica Sinica*, **1**(1), 67-72 (2010).

[10] Aggarwal R.C., Singh N.K., Prasad L., Complexes of benzoylisonicotinic acid hydrazide with VO(II), Mn(II), Co(II), Ni(II), Cu(II) and Zn(II), *Ind. J. Chem. Sec A* **14** (3), 181-183 (1976).

[11] Maiti A., Ghosh S., Synthesis and Reactivity of some octacoordinated Dioxouranium (VI) Complexes of Diacetyl bis(benzoylhydrazone) and Benzil bis (benzoylhydrazone), *Indian J Chem*., **28**(11), 980-983 (1989).

[12] Aggarwal R.C., Singh N.K., Singh R.P., Synthesis and structural studies of some 1st row transition-metal complexes of salicylaldehyde hydrazone, *Inorg. Chim. Acta* **32** (2), 87-90 (1979).

[13] Singh N.K., Srivastva S.C., Aggarwal R.C., Studies on 3d-metal complexes of acetylacetone ethoxythiocarbonyl hydrazone, *J. Ind. Chem*. **60** (7), 622-624 (1983).

[14] Agarwal R.K., Sarin R.K., Synthesis and characterization of some lanthanide(III) perchlorate complexes of hydrazones of isonicotinic acid hydrazide, *Polyhedron*, **12**(19), 2411-2415 (1993).

[15] Bhaskar R., Salunkhe N., Yaul A., Aswar A., Bivalent transition metal complexes of ONO donor hydrazone ligand: Synthesis, structural characterization and antimicrobial activity. *Spectrochim. Acta A Mol. Biomol. Spectrosc.* **151**, 621–627 (2015).

[16] Ayyannan G., Mohanraj M., Raja G., Bhuvanesh N., Nandhakumar R., Jayabalakrishnan C., New palladium(II) hydrazone complexes: Synthesis, structure and biological evaluation, *J. Photochem. Photobio. B Biol.* **163**, 1-13 (2016).

[17] Xu J., Zhou T., Xu Z.Q., Gu X.N., Wu W.N., Chen H., Wang Y., Jia L., Zhu T.F., Chen R.H., Synthesis, crystal structures and antitumor activities of copper(II) complexes with a 2-acetylpyrazine isonicotinoyl hydrazone ligand, *J. Mol. Struct*. **11**(28), 448–454, (2017).

[18] Mohanraj M., Ayyannan G., Raja G., Jayabalakrishnan C., Synthesis , spectral characterization, DNA interaction, radical scavenging and cytotoxicity studies of ruthenium(II) hydrazone complexes, *J. Photochem. Photobio. B Biol.* **158**, 164-173, 2016.

[19] Cozzi P.G., Metal–Salen Schiff base complexes in catalysis: practical aspects, *Chem. Soc. Rev*., **33**, 410-421 (2004).

[20] Ayyannan G., Mohanraj M., Raja G., Bhuvanesh N., Nandhakumar R., Jayabalakrishnan C., Design, synthesis, structure and

biological evaluation of new palladium(II) hydrazone complexes, *Inorg.Chim. Acta*. **453**, 562-573 (2016).

[21] Singh Y.P., Patel R.N., Singh Y., Butcher R.J., Vishakarma P.K., Singh R.K.B., Structure and antioxidant superoxide dismutase activity of copper(II) hydrazone complexes, *Polyhedron* **122**,.1-15 (2017).

[22] Rodic M.V., Leovac V.M., Jovanovic L.S., Spasojevic V., Joksovic M.D., Stanojkovic T., Matic I.Z., Vojinovic -Ješic L.S., Markovic V., Synthesis, characterization, cytotoxicity and antiangiogenic activity of copper(II) complexes with 1-adamantoyl hydrazone bearing pyridine rings, *Eur. J. Med. Chem.* **115**, 75-81 (2016).

[23] Ragavendran J.V., Sriram D., Patel S.K., Reddy I.V., Bharathwajan N., Stables J., Yogeeswari P., Design and synthesis of anticonvulsants from a combined phthalimide-GABA-anilide and hydrazone pharmacophore, *Eur.J.Med.Chem.* **42**, 146-151(2007).

[24] Joshi S.D., KumarD., Dixit S.R., Tigadi N., Lherbet C., Aminabhavi T.M., Yang K.S., Synthesis, characterization and antitubercular activities of novel pyrrolyl hydrazones and their Cu-complexes, *Eur. J. Med. Chem.* **121**, 21-39 (2016).

[25] Rollas S., Küçükgüzel S.G., Biological activities of hydrazone derivatives, *Molecules*. **12**(8), 1910-1939 (2007).

[26] El-Saied F.A., Ayad M.I., Yousef O., Farid R.W., Spectroscopic Characterization and Biological activity of metal complexes of N' -(dibenzoylacetone -2- ylmethylene) 2(4-methylphenylamino)acetohydrazide, Smart *Nanocomposites*. **1**(2), 141-161 (2011).

[27] Liu M., Wang Y., WangYang W.Z., Liu F., Cui Y.L., Duan Y.S., Wang M., Liu S.Z., Rui C.H., Design, synthesis, and insecticidal activities of phthalamides containing a hydrazone substructure, *J. Agric. Food Chem*., **58**(11), 6858-6863 (2010).

[28] Wu J., Song B.A., Hu D.Y., Yue M., Yang S., Design, synthesis and insecticidal activities of novel pyrazole amides containing hydrazone substructures, *Pest Manag. Sci.* **68**(5), 801-810 (2011).

[29] El-Saied F. A., Aly S.A., Salem T.A., Synthesis, characterization of vanadium complexes and evaluation their anti-hyperglycemic effect, *J. Chem. Pharm. Res*., **8**(8), 171-181 (2016).

[30] Ibrahim K.M., Gabr I.M., Zaky R.R., Synthesis and magnetic, spectral and thermal eukaryotic DNA studies of some 2-acetylpyridine-[N-(3-hydroxy-2-naphthoyl)] hydrazone complexes., *J. Coord. Chem*., **62**(7), 1100-1111 (2009).

[31] El-Behery M., El-Twigry H., Synthesis, magnetic, spectral, and antimicrobial studies of Cu(II), Ni(II) Co(II), Fe(III), and UO2(II) complexes of a new Schiff base hydrazone derived from 7-chloro-4-hydrazinoquinoline, *Spectrochim Acta (A),* **66** (1), 28-36 (2007).

[32] Pouralimardan O., Chamayou A.C., Janiak.C., Monfared H.H., Hydrazone Schiff base-manganese (II) complexes: Synthesis, crystal structure and catalytic reactivity, *Inorg. Chim. Acta*, **360**(5),1599-1608 (2007).

[33] Ghorbanloo M., Jafari S., Bikas R., Krawczyk M.S., Lis T., Dioxidovanadium(V) complexes containing thiazol-hydrazone NNN-donor ligands and their catalytic activity in the oxidation of olefins, *Inorg. Chim. Acta*, **455** , 15-24 (2017).

[34] Zhang Y., Yang T., Zheng B.Y., Liu M.Y., Xing N., Synthesis, crystal structures of oxovanadium(V) complexes with hydrazone ligands and their catalytic performance for the styrene oxidation. *Polyhedron* **121**, 123-129 (2017).

[35] Basu C., Chowdhury S., Banerjee R., Evans H.S., Mukherjee S., A novel blue luminescent high-spin iron(III) complex with interlayer O-H…Cl bridging: Synthesis, structure and spectroscopic studies, *Polyhedron*. **26**(14), 3617–3624 (2007).

[36] Bakir M., Green O., Mulder W.H., Synthesis, characterization and molecular sensing behavior of [ZnCl2 (η 3-N, N, O-dpkbh)](dpkbh=di-2-pyridyl ketone benzoyl hydrazone . *J. Mol. Struct*., **873**(1), 17-28 (2008).

[37] Hussain M.S., Rehman S.U.Z., Synthesis and Characterization of Ni(II), Cu(II) and Zn(II) Tetrahedral Transition Metal Complexes of Modified Hydrazine, *Naturforsch.* **33**(b), 67-71 (1978).

[38] Richardson D.R., Iron chelators as therapeutic agents for the treatment of cancer , Crit. Rev. Oncol. *Hematol*. **42**, 267–281 (2002).

[39] Hussain M.S., Rehman S.U., Synthesis and Biological Studies of Complexes of 2- amino-N(2-aminobenzoyl) Benzohydrazide with Co(II), Ni(II), and Cu(II), *Inorg. Chim. Acta*, **60**, 231-238 (1982).

[40] El-Gammal O.A., Rakha T.H., Metwally H.M., Abu El-Reash G.M., Synthesis, characterization, DFT and biological studies of isatinpicolinohydrazone and its Zn(II), Cd(II) and Hg(II) complexes. *Spectrochim Acta Part A Mol. Biomol. Spectrosc.* **127**, 144-156 (2014).

[41] El-Saied F.A., Shakdofa M.M.E., El-Tabl.A.S., Elzaher M.M.A., Coordination behaviour of N'1,N'4-bis((1,5-dimethyl-3-oxo-2-phenyl-2,3-dihydro-1H-pyrazol-4-yl)methylene) succinohydrazide toward transition metal ions and their antimicrobial activities, *Main Group Chem.* **13**, 87-103 (2014).

[42] Galal S.A., Hegab K.H., Kassab A.S., Rodriguez M.L., Kerwin S.M., El Khamry A. M.A., Diwani H.I., New transition metal ion complexes with benzimidazole-5-carboxylic acid hydrazides with antitumor activity, *Eur. J. Med. Chem*., **44**, 1500-1508 (2009).

[43] Sivaramaiah S., Reddy P.R., Direct and derivative spectrophotometric determination of zinc with 2,4-dihydroxybenzaldehyde isonicotinoyl hydrazone in potable water and pharmaceutical samples, *J. Anal. Chem.* **60**(9), 828-832, (2005).

[44] Vargas M.G., Trevilla S., Milla M., Synthesis and characterization of 1,2- cyclohexanedione

bis-benzoyl-hydrazone and its application to the determination of ti in minerals and rocks, *Talanta*. **33**(3), 209-214 (1986).

[45] Fouda M.F.R., Abd-Elzaher M.M., Shakdofa M.M.E., El-Saied F.A., Ayad M.I., El-Tabl A.S., Synthesis and characterization of transition metal complexes of N'- [(1,5-dimethyl-3-oxo-2-phenyl-2,3-dihydro-1H-pyrazol-4-yl)methylene] thiophene-2-carbohydrazide. *Transition Met. Chem*. **33**, 219-228 (2008) .

[46] Ahmed R.A. Lal, Synthesis, characterization and electrochemical studies of copper(II) complexes derived from succinoyl- and adipoyldihydrazones , *Arab. J. Chem*. **10**, S901–S908 (2017).

[47] Roe R.R., Pang Y., Zinc′s Exclusive Tetrahedral Coordination Governed by Its Electronic Structure, *J. Mol. Model.* **5**, 134-140 (2009).

[48] El-Saied F.A., Salem T.A., El-Aarag B.Y., Hashim M.A., Synthesis, Characterization and Biological Evaluation of Metal Complexes Derived from 2-(phenylamino)acetohydrazide ligand, *European Journal of Pharmaceutical and Medical Research*. **5**(6),120- 134 (2018).

[49] Para S., Karolczyk-Kostuch S., Fiedorowicz M., Dihydrazone of dialdehyde starch and its metal complexes, *Carbohydr. Polym*. **56**, 187-193 (2004).

[50] El-Saied F.A., Shakdofa M.M.E., El Tabl A.S., Abd-Elzaher M.M., Morsy N., Coordination versatility of N2O4 polydentate hydrazonic ligand in Zn(II), Cu(II), Ni(II), Co(II), Mn(II) and Pd(II) complexes and antimicrobial evaluation, *J. Basic Appl. Sci.* **6** ,310-320 (2017).

[51] Rollas S., Küçükgüzel Ş.G., Biological activities of hydrazone derivatives, *Molecules* **12**(8):1910–1939 (2007).

[52] Şenkardeş S., Kaushik-Basu N., Durmaz I., Manvar D., Basu A., Atalay R.,. et al. Synthesis of novel diflunsiahydrazide-hydrazones as anti-hepatitis C virus agents and hepatocellular carcinoma inhibitors. *Eur. J. Med. Chem.* **108**, 301–308 (2016).

[53] Zhang D., Ma Y., Liu Y., Liu ZP., Synthesis of sulfonylhydrazone- and acylhydrazone-substituted 8-ethoxy-3- nitro-2H-chromenes as potent antiproliferative and apoptosis inducing agents. *Arch Pharm (Weinheim)* **8 ,**576–588 (2014).

[54] Dandawate P., Khan E., Padhye S., Gaba H., Sinha S., Deshpande J.,et al. Synthesis, characterization, molecular docking and cytotoxic activity of novel plumbagin hydrazones against breast cancer cells. *Bioorg Med Chem Lett*. **22** , 3104–3108(2014) .

[55] Mohareb R.M., Al-Omran F., Reaction of pregnenolone with cyanoacetylhydrazine: Novel synthesis of hydrazide-hydrazone, pyrazole, pyridine, thiazole, thiophene derivatives and their cytotoxicity evaluations. *Steroids*. **77**, 1551–1591 (2012).

[56] Aydýn S., Kaushik-Basu N., Arora P., Basu A., Nichols B.D., Talele T.T., et al. Microwave assisted synthesis of some novel flurbiprofen hydrazidehydrazones as anti-HCV NS5B and anti-cancer agents. *Marmara Pharm J.* **17** ,26–34 (2013).

[57] Cui Z., Li .Y., Ling Y., Huang J., Cui .J., Wang R., et al. New class of potent antitumor acylhydrazone derivatives containing furan. *Eur.J.Med.Chem*. **45**, 5576–84 (2010).

[58] Al-Said M.S., Bashandy M.S., Al-Qasoumi S.I., Ghorab M.M., Anti-breast cancer activity of some novel 1,2-dihydropyridine, thiophene and thiazole derivatives. *Eur. J. Med. Chem*. **46**, 137–141 (2011)

[59] Liu T., Sun C., Xing X., Jing L., Tan R., Luo Y., et al. Synthesis and evaluation of 2-[2-(phenylthiomethyl)-1H-benzo[d] imidazol-1-yl) acetohydrazide derivatives as antitumor agents. *Bioorg.Med.Chem. Lett*. **22**, 3122–3125 (2012).

[60] Despaigne A.A., Parrilha G.L., Izidoro J.B., Da Costa P.R., Dos Santos R.G., Piro O.E., et al. 2-Acetylpyridine-and 2-benzoylpyridine-derived hydrazones and their gallium (III) complexes are highly cytotoxic to glioma cells. *Eur. J. Med. Chem*. **50**, 163–172 (2012) .

[61] Abdel-Aziz A.A.M., El-Azab A.S., AlSaif N.A., Obaidullah A.J., Al-Obaid A.M., Al-Suwaidan J.I.A., Synthesis, potential antitumor activity, cell cycle analysis, and multitarget mechanisms of novel hydrazones incorporating a 4-methylsulfonylbenzene scaffold: a molecular docking study**,** *Enzyme Inhib. Med. Chem.*, **22** , 63–80 (2021).

[62] Sonia S., Asija S., Kumar N., Deswal Y., Devi J., Organotin (IV) complexes derived from tridentate Schiff base ligands: Synthesis, spectroscopic analysis, antimicrobial and antioxidant activity, Journal of the *Indian Chemical Society*, **99**(3), 100379 (2022).

[63] Kumar N., Asija S., Deswal Y., Saroya S., Kumar A., Devi J., Organotin(IV) complexes derived from hydrazone ligands: Synthesis, spectral analysis, antimicrobial and molecular docking studies, *Phosphorus, Sulfur, and Silicon and the Related Elements*, 197: **9**, 952-963 (2022) .

[64] Saroya S., Asija S., Deswal Y., et al , Synthesis, spectral studies, in vitro antimicrobial activity and molecular docking studies of organotin(IV) complexes derived from tridentate Schiff base ligands, *Res Chem Intermed* **48**, 2949–2971 (2022).

[65] El-Aarag B., El-Saied F.A., Salem T., Khedr N., Khalifa S.H., El-Seedi H.R., New metal complexes derived from diacetylmonoxime-n(4)antipyrinylthiosemicarbazone: Synthesis, characterization and evaluation of antitumor activity against Ehrlich solid tumors induced in mice, *Arab. J. Chem.*, **14**, 93-102 (2021) .

[66] El-Saied F.A., El-Aarag B., Salem T., Said G.H., Khalefa S.H., El-Seedi H., Synthesis, characterization and antitumor activity of metal complexes derived from isatin-N(4)antipyrinethiosemicarbazone ligand against Ehrlich ascites carcinoma cells, *Molecules*, **24**(18), 3313 (2019).

[67] EL-Saied F.A., Shakdofa M.M.E., Al-Hakimi A.N., Synthesis, Characterization and Antimicrobial Activities of Hydrazone Ligands Derived from 2-(phenylamino)acetohydrazide and Their Metal Complexes, *Journal of the*

Korean Chemical Society, **55** (3),444- 453 , (2011).

[68] Emam S.M., AbouEl-Enein S.A., El-Saied F.A., Alshater S.Y., Synthesis and characterization of some bi, tri and tetravalent transition metal complexes of N' -(furan-2-yl-methylene)-2-(p-tolylamino)acetohydrazide HL1 and N' -(thiophen-2-yl-methylene)-2-(p-tolylamino)acetohydrazide HL2 , *Spectro. Chim. Acta part A*, **92**, 96-104, (2012).

[69] El-Saied F.A., El-Asmy A.A., Kaminsky W., West D.X., Spectral and structural studies of cobalt (II, III), nickel (II), and copper (II) complexes of dehydroacetic acid N4-dialkyl- and 3-azacyclothiosemicarbazones, *Transition metal chemistry*, **28**, 954-960 (2003) .

[70] EL-Tabl A.S., EL-Saied F.A., AL-Hakimi A.N., Synthesis, spectroscopic investigation and biological activity of metal complexes with ONO trifunctionalalized hydrazone ligand, *Transition Metal Chemistry*, **32**, 689–701 (2007).

[71] Devi J., Devi S., Kumar A., Synthesis, characterization, and quantitative structure–activity relationship studies of bioactive dehydroacetic acid and amino ether Schiff base complexes, *Heteroatom Chemistry*, **27**, 361-371(2016).

[72] El-Aarag B.Y., Kasai T., Zahran M.A., Zakhary N.I., Shigehiro T., Sekhar S.C., Agwa H.S., Mizutani A., Murakami H., Kakuta H., Seno M., In vitro anti-proliferative and anti-angiogenic activities of thalidomide dithiocarbamate analogs. *Int Immunopharmacol*. **21**(2), 283-292 (2014).

[73] El-Aarag B., Kasai T., Masuda J., Zahran M., Agwa H., Seno M., Anticancer effects of novel thalidomide analogs in A549 cells through inhibition of vascular endothelial growth factor and matrix metalloproteinase-2. *Biomedicine & Pharmacotherapy*, **85** ,549–555 (2017).

[74] Deswal Y., Asija S., Tufail A., Dubey A., Deswal L., Kumar N., Saroya S., Kirar J.T. S., Gupta N.M. Instigating the in vitro antidiabetic activity of new tridentate Schiff base ligand appended M(II) complexes: From synthesis, structural characterization, quantum computational calculations to molecular docking, and molecular dynamics simulation studies. *Applied Organometallic Chemistry*, **37** , 99 -112(2023).

[75] Deswal Y., Asija.S., Dubey A., Deswal L., Kumar D., Jindal D.K., Devi J., Cobalt(II), nickel(II), copper(II) and zinc(II) complexes of thiadiazole based Schiff base ligands: Synthesis, structural characterization, DFT, antidiabetic and molecular docking studies, *Journal of Molecular Structure*, **66**, 1253-1322 (2022).

[76] Deswal, Y., Asija, S., Kumar, D. et al. Transition metal complexes of triazole-based bioactive ligands: synthesis, spectral characterization, antimicrobial, anticancer and molecular docking studies. *Res.Chem. Intermed.*, **48**, 703–729 (2022).

[77] Nakamoto K., Infrared Spectra of Inorganic and Coordination Compounds, Wiley Interscience, New York, **35** ,137- 150 (1970).

[78] Murukan B., Mohanan.K., Synthesis, Characterization, Electrochemical Properties and Antibacterial Activity of Some Transition Metal Complexes with [(2-hydroxy-1-naphthaldehyde)-3- isatin]-bishydrazone, *Transition Met.Chem.*, vol. **31**, 441-446 (2006).

[79] Nakamoto K., Infrared and Raman Spectra of Inorganic and Coordination Compounds, *Wiley Interscience, New York*, **41**(16), 2290–2340(1986).

[80] Nakamoto K., Infrared and Raman Spectra of Inorganic and Coordination Compounds Part B: Applications in Coordination, *Organometallic, and Bioinorganic Chemistry*.John Wiley & Sons INC, USA, **8**(7), 380–401 (2009).

[81] El-Tabl A.S., El-Saied F.A., Al-Hakimi A.N., Spectroscopic characterization and biological activity of metal complexes with an ONO trifunctionalized hydrazone ligand, *J.Coordination Chemistry*, **61**(15), 2380–2401 (2008).

[82] Kavitha N., Anantha Lakshmi.P.V., Synthesis, characterization, thermal and 3D molecular modeling studies of transition metal complexes supported by ONN/ONO tridentate Schiff base hydrazone, *Der Pharma Chemica*, **8** (12),184-197 (2016).

[83] Alhadi A.A., Shaker S.A., Suleiman N., Wagee G., Yehye A., Ali H.M., Preparation, spectroscopic characterization of a new Cd(II) complex containing tridentate NNO schiff base derived and x-ray crystallographic structural study of 3,4,5- trihydroxybenzoic acid[1-(pyridyl)-ethylidene] hydrazone, *J. Chil. Chem. Soc*. **57** , 1283-1286 (2012).

[84] Lever A.B.P., Inorganic Electronic Spectroscopy, Elsevier, Amsterdam , **275** (1968).

[85] Patange V.N., Arbad B.R., Mane V.G., Salunke S.D., Synthesis, physico-chemical and antimicrobial screening studies of some transition metal complexes with O:O donor ligands, *Transition Metal Chemistry*, **32**, 944–949 (2007).

[86] Ahonțu E., Ilieș C.D., Shova S., Oprean C., Păunescu V., Olaru O.T., et al. Synthesis, Characterization, Antimicrobial and Antiproliferative Activity Evaluation of Cu(II), Co(II), Zn(II), Ni(II) and Pt(II) Complexes with Isoniazid-Derived Compound, *Molecules*, **22**(4),650 (2017).

[87] El-Sawaf A.K., West D.X., El-Saied F.A., El-Bahnasawy R.M., Synthesis, magnetic and spectral studies of iron(III), cobalt(II,III), nickel(II), copper(II) and zinc(II) complexes of 4–formylantipyrine N(4)-antipyrinylthiosemicarbazone, *Transition Met, Chem.*, **23**, 649−655 (1998).

[88] Lever A.B.P., Inorganic Electronic Spectroscopy, Studies in Physical and Theoretical Chemistry, *Science*. **25** , 123- 129 (1984).

[89] Mangalam N.A., Prathapachandra Kurup M.R., Versatile binding properties of a di-2-pyridyl ketone nicotinoylhydrazone ligand: Crystal structure of a Cu(II) complex,

Spectrochim, *Acta Part A Mol. Biomol. Spectros.*, **78**, 926–934 (2011).
[90] El-Saied F.A., El-Asmy A.A., Kaminsky W., West D.X., Spectral and structural studies of cobalt (ii,iii), and copper (ii) complexes of dehydroacetic acid N_4 – dialkyl – and 3 – azoacyclothio semicarbazones, *Transition Met.Chem*., **28**, 954 (2003**)**.
[91] El-Tabl A.S., Shakdofa M.M.E., El-Seidy A.M.A., Al-Hakimi A.N., Synthesis, characterization and antifungal activity of metal complexes of 2-(5-((2chlorophenyl) diazenyl) -2-hydroxybenzylidene) hydrazinecarbothioamide, *Phosphorus Sulfur Silicon Relat. Elem.* **187**, 1312-1323 (2012).
[92] Kasumov V.T., Köksal F., Synthesis, ESR, UV-Visible and reactivity studies of new bis(N-dimethoxyaniline-3,5-(t)Bu2-salicylaldiminato)copper(II) complexes. *Spectrochim, Acta Part A Mol. Biomol. Spectrosc.* ***98***, 207 (2012).
[93] Hathaway B.J., Billing D.E., The electronic properties and stereochemistry of mono-nuclear complexes of the copper(II) ion, *Coord. Chem. Rev*., **5**, 1949 (1970).
[94] Zaky R.R., Ibrahim K.M., Gabr I.M., Bivalent transition metal complexes of o-hydroxyacetophenone [N-(3-hydroxy-2-naphthoyl)] hydrazone: Spectroscopic, antibacterial, antifungal activity and thermogravimetric studies, *Spectrochim. Acta Part A Mol. Biomol. Spectrosc.*, ***81***, 28 (2011).
[95] Brown D.R., West D. X., An ESR study of addition species formed between bis(2-thiopyridine N-oxide)Cu(II) and heterocyclic and aliphatic amines, *J. Inorg. Nucl. Chem.*, ***43***, 1017 (1981).
[96] Nagashri K., Joseph J., Dhanaraj C.J., Nagashri K., Joseph J., Dhanaraj C.J., Copper (II) complexes of hydroxyflavone derivatives as potential bioactive molecule to combat antioxidants: Synthesis, characterization and pharmacological activities, *Appl. Organomet. Chem.*, ***25***, 704-717 (2011**)**.
[97] Proctor I.M., Hathaway B.J., Nicholis P., The electronic properties and stereochemistry of the copper(II) ion. Part I. Bis(ethylenediamine)copper(II) complexes, *J. Chem. Soc* **150**, 1678 (1968).
[98] Kivelson D., Neiman R., ESR Studies on the Bonding in Copper Complexes, *The Journal of Chemical Physics*, ***35***, 149 (2004).
[99] Kamatchi T.S., Subarkhan M.K., Ramesh R., Wang H. and Małeckic J.G., Investigation into antiproliferative activity and apoptosis mechanism of new arene Ru(II) carbazole-based hydrazone complexes, *Dalton Trans*., **49**, 11385 (2020).
[100] Elsayed S.A., Elnabky I.M., diBiase A., El-Hendawy A.M., New mixed ligand copper(II) hydrazone-base complexes: Synthesis, characterization, crystal structure, DNA/RNA/BSA binding, in vitro anticancer, apoptotic activity, and cellcycle analysis. *Appl.Organomet.Chem*., **36**(1), e6481 (2022).